FRPRCS-6 Conference, Singapore, 8 – 10 July 2003

THE BILINEAR STRESS-SLIP BOND MODEL: THEORETICAL BACKGROUND AND SIGNIFICANCE

T. ULAGA AND T. VOGEL

Institute of Structural Engineering (IBK), ETH Zurich, Hoenggerberg, 8093 Zurich, Switzerland

U. MEIER

Swiss Federal Laboratories for Materials Testing and Research (EMPA), Ueberlandstrasse 129, 8600 Duebendorf, Switzerland

Bond is the basic property that enables a successful strengthening of concrete structures with CFRP plates. In order to find an appropriate way to investigate arbitrary bond situations some micromechanical considerations are presented first. With transparent models it is possible to derive the hardening behaviour "at low load" and the softening behaviour "at high load". The latter situation is characterized by the presence of a crack which has a weakening effect. The simplest way to idealize these findings is a bilinear stress-slip relationship. With this tool bond problems can be treated mathematically. In the case of anchorage capacity considerations some simple but very useful formulas can be derived. Finally, a good agreement between theoretical and experimental results can be found.

INTRODUCTION

The application of externally bonded steel plates for the strengthening of reinforced concrete structures was already widespread in the 1970s. In the 80s and 90s research projects aimed at establishing the use of carbon fibre-reinforced plastic plates for the same purpose. Since then, this strengthening method has been used even more often and today many applications can be found.

The interaction between the components concrete and plate reinforcement requires the presence of a sufficient bond which enables the transfer of forces. In many practical cases, the existence of this property is considered as given and no further investigations are performed. In fact, there are only few scientifically established but applicable approaches which help to treat this question[1].

In order to characterize the bond properties a stress-slip relationship can be used. When the curve is simple but still sufficiently considers the real behaviour it can be used as a powerful tool for a variety of bond considerations.

BOND ANALYSIS

"Bond at low load"

Basics

Figure 1(a) displays a CFRP plate–concrete bond situation "at low load". A slip displacement, s_l, of the two elements is possible due to shear deformations in the adhesive layer.

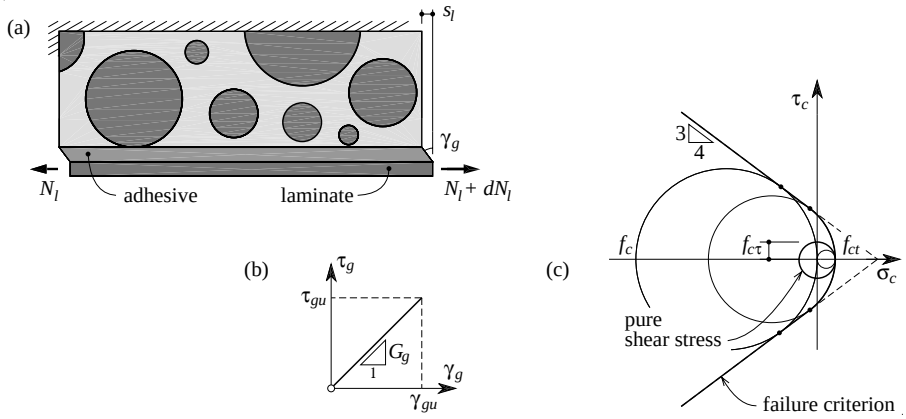

Figure 1: "Bond at low load"

Assumptions

The shear deformations are considered to be concentrated in the adhesive layer only. The corresponding shear stress–shear strain relationship is given in Figure 1(b). A continuous increase of the load will cause the sudden development of a crack in the weakest element, i.e. in the concrete body. When this occurs the bond situation turns into that of "bond at high load".

Modelling

With the diagram in Figure 1(b) the slip, s_l, can be determined according to Eq. (1). A crack in the concrete body will start to grow when

the shear stress τ_{l0} is achieved. This stress is related to the concrete shear strength, $f_{c\tau}$, which can be estimated with the modified Coulomb failure criterion[2] in Figure 1(c). With Eq. (2) it is possible to consider the fact that τ_{l0} is focused on one particular location and therefore generally will be slightly higher than $f_{c\tau}$ or f_{ct}, respectively.

$$s_l = \frac{t_g}{G_g} \cdot \tau_l \tag{1}$$

$$\tau_{l0} = a \cdot f_{c\tau} = a \cdot f_{ct} \qquad a \geq 1.0 \tag{2}$$

"Bond at high load"

Basics

In Figure 2(a) a longitudinal section through a CFRP plate-strengthened concrete beam is given. A crack plane has separated the plate from the body, therefore the situation can be considered as "bond at high load". Apparently the increase of the slip, s_l, also requires an increase of the crack width, w_r. In order to model the geometry of this process a simple assumption appears to be appropriate: the displacement of the crack faces is governed by an inclined opening where the angle α is the decisive parameter. For compatibility reasons the aggregate particles cause local abrasion effects in the matrix of the opposite crack face. This aggregate interlock mechanism enables the transfer of bond forces across the crack plane.

The analysis of aggregate interlock mechanisms was investigated by Walraven[3]. He established a closed-form mathematical model which he used to determine bond stresses in specimens which were subjected to pure shear load. In the case of the present considerations the displacement process is different, so that the Walraven theory must be modified in order to find an appropriate bond stress model.

Assumptions

The concrete body consists of perfectly spherical aggregate particles which are embedded in a cement matrix. The aggregate ratio, ρ_a, is defined according to Eq. (3) and the distribution of the diameters is described by the Fuller function, Eq. (4).

$$\rho_a = \frac{V_a}{V_c} \tag{3}$$

$$a_F(d) = \sqrt{\frac{d}{d_{\max}}} \tag{4}$$

The abrasion of the matrix causes normal and shear stresses, σ_{mu} and τ_{mu}, in the cement-aggregate contact zone, Figure 2(b). These stresses are connected according to Eq. (5) and can be estimated corresponding to experimental results found by Walraven, Eq. (6).

$$\tau_{mu} = \mu \cdot \sigma_{mu} \tag{5}$$

$$\sigma_{mu} = 6.39 \cdot f_{cc}^{0.56} \qquad \mu = 0.4 \tag{6}$$

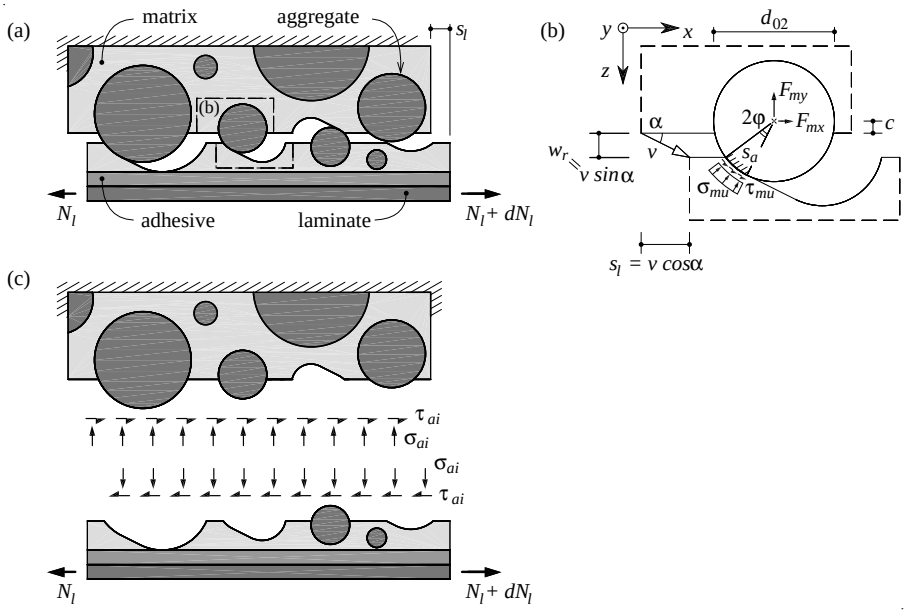

Figure 2: "Bond at high load"

Aggregate interlock theory in the case of an inclined crack opening: an overview

The crack faces contain aggregate particles which partly protrude from the cement matrix. The question that shall be treated in a first step is how many aggregate sphere caps can be expected to be found in a unit area of a crack face. For this purpose some probabilistic aspects need to be considered. The answer can be formulated as a probability density function for the two-dimensional case: Eq. (7) indicates the number of intersection circles with a diameter d_{02} which can be expected to be intersected by a horizontal unit length.

$$p_n = \frac{\frac{\partial}{\partial d_{02}} \left\{ \rho_a - \int_{d_{02}}^{d_{\max}} \left[\left(1 + \frac{1}{2} \cdot \left(\frac{d_{02}}{d_3} \right)^2 \right) \cdot \sqrt{1 + \left(\frac{d_{02}}{d_3} \right)^2} \cdot \frac{\rho_a}{2 \cdot \sqrt{d_{\max} \cdot d_3}} \right] \partial d_3 \right\}}{\frac{1}{4} \cdot d_{02} \cdot \pi} \quad (7)$$

In a second step the geometry and the stresses of the contact zone of an intersection circle with a diameter d_{02} will be studied, Figure 2(b). When the length and the angle of an opening vector, v and α, are given and the embedment depth of the intersection circle, c, is known, the contact angle, φ, can be determined from Eq. (8). The most probable contact angle, $\bar{\varphi}$, follows from Eq. (9). Integration of the stresses in the contact zone will provide the interlock forces of the considered intersection circle, Eq. (10) and (11).

$$\sin(2 \cdot \varphi) = \sqrt{1 - \left(2 \cdot \frac{v \cdot \sin\alpha + c}{d_{02}} \right)^2} \cdot \cos\alpha - \left(2 \cdot \frac{v \cdot \sin\alpha + c}{d_{02}} \right) \cdot \sin\alpha \quad (8)$$

$$\bar{\varphi} = \int_{c_{\min}=0}^{c_{\max}=\frac{d_{02} \cdot \cos\alpha}{2}} \left(\frac{2}{d_{02}} \cdot \varphi \right) \partial c \quad (9)$$

$$F_{mx}(\varphi) = d_{02} \cdot \sigma_{mu} \cdot \sin\varphi \cdot [\sin(\alpha + \varphi) + \mu \cdot \cos(\alpha + \varphi)] \quad (10)$$

$$F_{mz}(\varphi) = d_{02} \cdot \sigma_{mu} \cdot \sin\varphi \cdot [\cos(\alpha + \varphi) - \mu \cdot \sin(\alpha + \varphi)] \quad (11)$$

The third step aims at combining the single aspects that were treated before. The global aggregate interlock stresses according to Figure 2(c), σ_{ai} and τ_{ai}, can be determined by multiplication of p_n and F_{mx} or F_{mz}, respectively, and integration over the entire aggregate diameter range, Eq. (12).

$$\sigma_{ai} = \int_{d_{\min}=0}^{d_{\max}} p_n \cdot F_{mz}(\bar{\varphi}) \partial d_{02} \qquad \tau_{ai} = \int_{d_{\min}=0}^{d_{\max}} p_n \cdot F_{mx}(\bar{\varphi}) \partial d_{02} \quad (12)$$

Parameters

In order to evaluate the theoretical aggregate interlock model a set of parameters must be defined. The aggregate ratio, ρ_a, and the maximum aggregate size, d_{max}, are geometrical parameters that describe the architecture of the concrete structure. In the vicinity of the concrete surface

large aggregate particles are missing, therefore the depth of the crack plane, t, is of major significance. In the present considerations the concrete strength parameters f_{ct}, $f_{c\tau}$, f_{cc}, σ_{mu} and τ_{mu} are related to the concrete cylinder compressive strength, f_c, according to Eq. (13), (5) and (6). Finally, the crack opening vector, α, is used to characterize the inclination of the crack face displacement.

$$f_{ct} = f_{c\tau} = 0.3 \cdot f_c^{2/3} \qquad f_{cc} = 1.25 \cdot f_c \tag{13}$$

Stress-slip relationship: theoretically derived and idealized curve

The considerations that were presented before can be combined in order to obtain the stress-slip relationship in Figure 3(a). The parameters correspond to the average results from numerous experiments and can be considered as "reasonable" values, not as fixed constants.

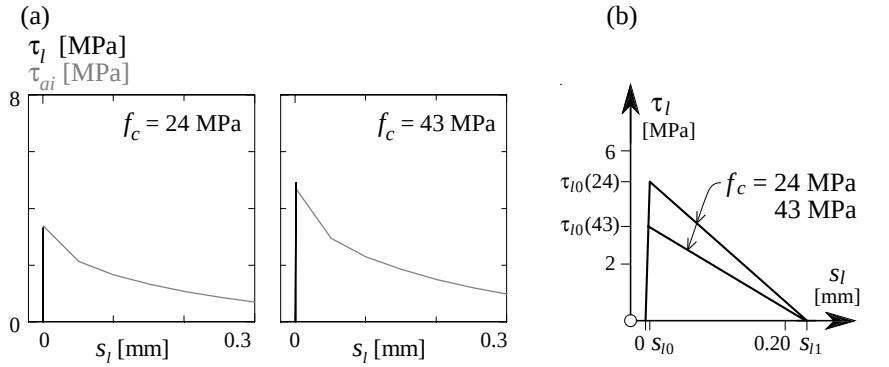

Model Parameters

"at low load": G_g = 10 GPa, t_g = 1 mm, a = 4/3

"at high load": ρ_a = 0.725, d_{max} = 8 mm, α = 45°, t = 1.5 mm

Characteristic parameters

$$\tau_{l0} = a \cdot f_{ct} = 0.4 \cdot f_c^{2/3} \tag{14}$$

$$s_{l0} = \frac{G_g}{t_g} \cdot \tau_{l0} \tag{15}$$

$$s_{l1} = s_{l0} + 0.225\,[mm] \tag{16}$$

Figure 3: Stress-slip relationships

In order to use the stress-slip relationship for theoretical investigations the curves in Figure 3(a) must be simplified. A good approximation can be achieved with the bilinear stress-slip relationship in Figure 3(b). The characteristic parameters of the hardening branch, τ_{l0} and s_{l0}, can be derived from the case "bond at low load", Eq. (14) and (15). The parameter of the softening branch, s_{l1}, was calibrated according to experimental results, Eq. (16), Figure 5.

SIGNIFICANCE

Theory

In Figure 4(a) a differential element of a tension chord reinforced with CFRP plates on two opposite faces is given. When concrete and plate display linear behaviour according to Figure 4(b), equilibrium and compatibility requirements result in the differential Eq. (17) [4]. The function $\tau_l(s_l)$ represents an arbitrary stress-slip relationship, Figure 4(c). It can be replaced by the bilinear stress-strain relationship in Figure 3(b) and the differential equation can be transformed into Eq. (18) and (19) which correspond to mathematical models for the hardening branch (index *I*) and the softening branch (index *II*), respectively. The integration of these equations provides the general solutions, Eq. (20) and (21). In the case of a particular bond problem the boundary conditions can be formulated in order to determine the coefficients *A*, *B*, *C* and *D*. With further calculations the stresses and strains can be derived easily.

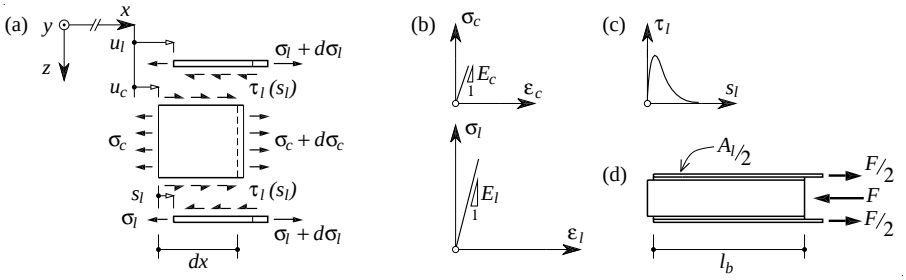

Figure 4: Theory basics

$$s_l'' - \frac{b_l \cdot (1 + n_l \cdot \rho_l)}{E_l \cdot A_l} \cdot \tau_l(s_l) = 0 \tag{17}$$

$$s_{II}'' - \omega^2 \cdot s_{II} = 0 \qquad \omega^2 = \frac{b_l \cdot (1 + n_l \cdot \rho_l)}{E_l \cdot A_l} \cdot \frac{\tau_{l0}}{s_{l0}} \tag{18}$$

$$s_{III}'' + \eta^2 \cdot s_{III} = \eta^2 \cdot s_{l1} \qquad \eta^2 = \omega^2 \cdot \frac{s_{l0}}{s_{l1} - s_{l0}} \tag{19}$$

$$s_{II}(x) = A \cdot \cosh(\omega x) + B \cdot \sinh(\omega x) \tag{20}$$

$$s_{III}(x) = C \cdot \cos(\eta x) + D \cdot \sin(\eta x) + s_{l1} \tag{21}$$

Anchorage capacity formulas

In Figure 4(d) a model of an anchorage situation is displayed. For practical dimensioning tasks it is important to know the capacity of such a detail. The basics that were given above can be applied to find very useful formulas. The admissible simplification according to Eq. (22) enables one to find the most efficient bond length, l_{b0}, Eq. (23). When the length of the bond zone is shorter, Eq. (24) indicates the bond capacity, F_b. When it is longer, the capacity remains constant according to Eq. (25), i.e. any lengthening beyond l_{b0} will bring no benefit. The specific bond fracture energy, G_{Fb}, corresponds to the area underneath the bilinear stress-slip curve and can be determined according to Eq. (26).

$$s_{l0} = 0 \tag{22}$$

$$l_{b0} = \frac{\pi}{2} \cdot \sqrt{\frac{2 \cdot E_l \cdot t_l \cdot G_{Fb}}{\left(1 + n_l \cdot \rho_l\right) \cdot \tau_{l0}^2}} \tag{23}$$

$$F_b\left(l_b < l_{b0}\right) = \sin \sqrt{\frac{\left(1 + n_l \cdot \rho_l\right) \cdot \tau_{l0}^2 \cdot l_b^2}{2 \cdot E_l \cdot t_l \cdot G_{Fb}}} \cdot b_l \cdot \sqrt{\frac{2 \cdot E_l \cdot t_l \cdot G_{Fb}}{\left(1 + n_l \cdot \rho_l\right)}} \tag{24}$$

$$F_b\left(l_b \geq l_{b0}\right) = b_l \cdot \sqrt{\frac{2 \cdot E_l \cdot t_l \cdot G_{Fb}}{\left(1 + n_l \cdot \rho_l\right)}} \tag{25}$$

$$G_{Fb} = \frac{\tau_{l0} \cdot s_{l1}}{2} \approx 0.045 \cdot f_c^{2/3} \tag{26}$$

Comparison with experiments

In Figure 5 a comparison between theory (according to Eq. (23)…(25)) and experimental bond capacity results is given. For this purpose tests by several authors were considered[4,5,6,7,8]. In all cases a set up similar to that in Figure 4(d) was used. In general a good agreement between theory and experiment can be observed.

Further potential

The derivation of anchorage capacity formulas represents one possible application of the bilinear stress-slip bond model. It can also be used for the examination of tension chords with mixed reinforcement: internal steel bars and external CFRP plates. The analysis provides crack distances, stresses and strains and bond coefficients. Hence, a variety of applications is possible.

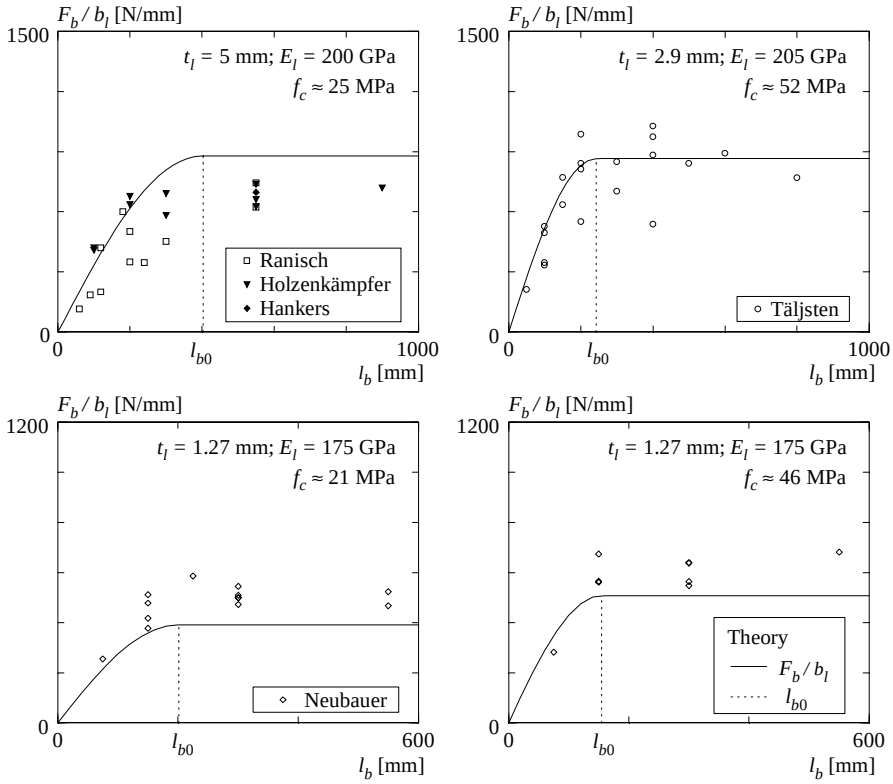

Figure 5: Comparison of theory and experiment

CONCLUSIONS

With mechanical bond analysis it is possible to derive the shape of the stress-slip relationship: a hardening branch turns into a softening branch when a crack occurs that weakens the bond structure.

A simple but appropriate idealization of the bond behaviour can be obtained with the bilinear stress-slip relationship.

The bilinear stress-slip relationship can be used for the mathematical investigation of various bond situations and therefore represents a powerful analysis tool.

NOTATION

Roman and Greek letters

A	area	v	vector length	*F*	Fuller; fracture	0	index
E	modulus of elasticity	w	crack width	*a*	aggregate	1	index
F	force	x	coordinate	*b*	bond	2	index
G	fracture energy; shear modulus	y	coordinate	*c*	concrete; cube	3	index
N	internal force	z	coordinate	*g*	adhesive	*I*	index
V	volume	α	angle	*i*	interlock	*II*	index
a	coefficient; distribution	γ	shear strain	*l*	plate		
b	width	ε	strain	*m*	matrix		
c	embedment depth	η	substitute	*max*	maximum		
d	diameter	μ	coefficient of friction	*min*	minimum		
f	strength	ρ	ratio	*n*	number		
l	length	σ	normal stress	*r*	crack		
n	modular ratio	τ	shear stress	*t*	tension		
s	slip; length	φ	angle	*u*	ultimate		
t	thickness; depth	ω	substitute	τ	shear		
u	displacement						

Subscripts

REFERENCES

1. Ulaga, T., Vogel, T., Meier, U.: *The premature Failure of CFRP laminate-Strengthened Concrete Structures*. Proceedings of the IABMAS'02 Conference, Barcelona, 2002, pp. 271…272.
2. Marti, P., Alvarez, M., Kaufmann, W., Sigrist, V.: *Tragverhalten von Stahlbeton*. IBK, ETH Zürich, Publikation SP-008, Sept. 1999, 301 pp.
3. Walraven, J. C.: *Aggregate Interlock: A Theoretical and Experimental Analysis*. PhD thesis, Delft University of Technology, Delft University Press, 1980, 197 pp.
4. Holzenkämpfer, P.: *Ingenieurmodelle des Verbunds geklebter Bewehrung für Betonbauteile*. DAfStb, Heft 473, Beuth Verlag GmbH, Berlin, 1997, pp. 109...209.
5. Hankers, Ch.: *Zum Verbundtragverhalten laschenverstärkter Betonbauteile unter nicht vorwiegend ruhender Beanspruchung*. DAfStb, Heft 473, Beuth Verlag GmbH, Berlin, 1997, pp. 7...107.
6. Neubauer, U., Rostasy, F. S.: *Bond Failure of Fiber Reinforced Polymer Plates at Inclined Cracks – Experiments and Fracture Mechanics Model*. Proceedings of the FRPRCS-4 Symposium, Baltimore, 1999, pp. 369…381.
7. Ranisch, E.-H.: *Zur Tragfähigkeit von Verklebungen zwischen Baustahl und Beton*. Dissertation, TU Braunschweig, Heft 54, 1982, 173 pp.
8. Täljsten, B.: Plate Bonding. Strengthening of Existing Concrete Structures with Epoxy Bonded Plates of Steel or Fibre Reinforced Plastics. Division of Structural Engineering. Lulea University, 190 pp.